Cell Reports

Article

Targeted Neurostimulation in Mouse Brains with Non-invasive Ultrasound

Graphical Abstract

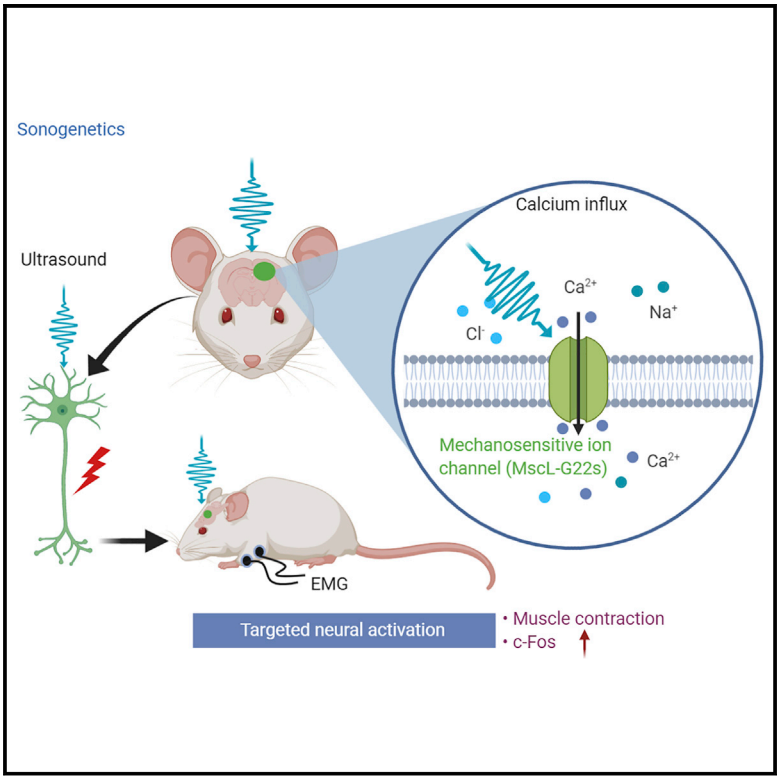

Authors

Zhihai Qiu, Shashwati Kala, Jinghui Guo, ..., Minyi Yang, Haoru Wang, Lei Sun

Correspondence

lei.sun@polyu.edu.hk

In Brief

Qiu et al. demonstrate a targeted sonogenetic approach: sensitizing neurons to low-intensity ultrasound stimulation by expressing the mechanosensitive channel MscL-G22S *in vitro* and *in vivo*. Ultrasound triggered Ca^{2+} influx-consequent neuronal activation in MscL-expressing cells. Transcranially stimulating MscL-expressing brain regions evoked muscular responses and c-Fos expression without widespread non-specific activation.

Highlights

- MscL-G22S expression efficiently sensitized cells to ultrasound stimulation
- Non-invasive ultrasound triggered neural activation in MscL-expressing regions
- Ultrasound targeted at the cortical M1 region with MscL evoked rapid EMG responses
- Ultrasound successfully activated MscL-expressing neurons in the deeper DMS region

Qiu et al., 2020, Cell Reports *32*, 108033
August 18, 2020
https://doi.org/10.1016/j.celrep.2020.108033

CellPress

Cell Reports

CellPress
OPEN ACCESS

Article

Targeted Neurostimulation in Mouse Brains with Non-invasive Ultrasound

Zhihai Qiu,[1,2] Shashwati Kala,[1,2] Jinghui Guo,[1,2] Quanxiang Xian,[1,2] Jiejun Zhu,[1] Ting Zhu,[1] Xuandi Hou,[1] Kin Fung Wong,[1] Minyi Yang,[1] Haoru Wang,[1] and Lei Sun[1,3,*]

[1]Department of Biomedical Engineering, The Hong Kong Polytechnic University, Hong Kong SAR, P. R. China, 999077

[2]These authors contributed equally

[3]Lead Contact

*Correspondence: lei.sun@polyu.edu.hk

https://doi.org/10.1016/j.celrep.2020.108033

SUMMARY

Recently developed brain stimulation techniques have significantly advanced our ability to manipulate the brain's function. However, stimulating specific neurons in a desired region without significant surgical invasion remains a challenge. Here, we demonstrate a neuron-specific and region-targeted neural excitation strategy using non-invasive ultrasound through activation of heterologously expressed mechanosensitive ion channels (MscL-G22S). Low-intensity ultrasound is significantly better at inducing Ca^{2+} influx and neuron activation *in vitro* and at evoking electromyogram (EMG) responses *in vivo* in targeted cells expressing MscL-G22S. Neurons in the cerebral cortex or dorsomedial striatum of mice are made to express MscL-G22S and stimulated ultrasonically. We find significant upregulation of c-Fos in neuron nuclei only in the regions expressing MscL-G22S compared with the non-MscL controls, as well as in various other regions in the same brain. Thus, we detail an effective approach for activating specific regions and cell types in intact mouse brains by sensitizing them to ultrasound using a mechanosensitive ion channel.

INTRODUCTION

Controlling local or global neuronal activity and signaling by physical intervention is a powerful way to gain causal insight into brain functions (Insel et al., 2013) and treat brain disorders (Anderson, 2012; Rajasethupathy et al., 2016). To achieve that, diverse modalities have been developed in the past few decades, including deep brain stimulation (DBS) (Lozano, 2017), transcranial direct (tDCS) and alternating (tACS) electric stimulation (Lang et al., 2004; Nitsche and Paulus, 2000), transcranial magnetic stimulation (TMS) (Okun, 2014), transcranial ultrasound brain stimulation (Legon et al., 2014), chemogenetics (Gomez et al., 2017), and optogenetics (Rajasethupathy et al., 2016). This has resulted in the rapid accumulation of knowledge about brain functions as well as treatment strategies for brain diseases (Insel et al., 2013; Leinenga et al., 2016). These findings have also, however, highlighted the need for stimulation techniques that possess cell-type or circuit-element specificity, high spatiotemporal resolution, brain-wide accessibility for local or global stimulation, and non-invasiveness for repeated implementation; all of which are crucial for fundamental research and clinical translation (Roy et al., 2016). These requirements being currently unmet, there is a strong impetus for new research techniques to be developed that can meet these goals.

Ultrasound-based stimulation is a promising candidate because it can potentially access deep brain structures non-invasively through the intact skull (King et al., 2013; Tufail et al., 2010) and be steered to millimeter-sized dynamic focal spots in deep brain regions (Legon et al., 2014). However, it is not currently able to target a desired population of neurons by cell-type, which could result in the dilution of its effects or even cause side-effects, depending on the application. Selectivity for cell types could be achieved through a strategy that confers ultrasonic sensitivity to targeted neurons, which could then allow ultrasonic control of neuronal activation and animal behavior, analogous to the optogenetic approach (Ibsen et al., 2015). This is potentially achievable through "mechanosensitive" ion channels, a crucial component of the cellular force-sensing machinery. The opening of these ion channels is controlled by diverse mechanical stimuli, such as touch, hearing, crowding, stretch, and cell volume, which convert physical force into cellular signaling (Martinac, 2012). Cellular mechanosensation through ion channels could thus serve as a mechanism used for ultrasonic stimulation of neurons.

Some previous studies have applied such an approach *in vitro* and *in vivo*. Ibsen et al. (2015) used low-frequency ultrasound in the presence of microbubbles, which served as acoustic actuators, to activate neurons overexpressing the TRP-4 channel in *Caenorhabditis elegans*, a method they termed "sonogenetics." More recently, Ye et al. (2018) used surface acoustic waves at ~30 MHz to activate a mutant version of the large conductance mechanosensitive ion channel (MscL-I92L) to facilitate stimulation of rat neurons *in vitro*. These studies demonstrated the activation of neuronal activity upon the application of ultrasound by overexpression of a mechanosensitive ion channel. Progressing from such studies of cells and lower-order animal models to application in the brains of mammals, however, would require some changes

to the approaches used previously. For one, intravascularly administered microbubbles used with lower-frequency ultrasound (Kubanek et al., 2016; Pan et al., 2018; Prieto et al., 2018) would be unsuitable to target a desired region of a mammalian brain because the large size of microbubbles prevents them from passing through blood vessels. Second, ultrasound frequencies would have to be lower to pass through the intact skull and stimulate neurons (Bystritsky and Korb, 2015; Tyler et al., 2018), but previous studies of the effects of ultrasound alone on cultured cells tend to use high frequencies. An approach possessing the ability to successfully pass through the intact skull and to stimulate only a desired region or cell type would provide a very useful tool with which to study the brain. It is, therefore, compelling to examine whether expressing mechanosensitive ion channels in mammalian neurons and stimulating them with low-intensity, low-frequency ultrasound could constitute an efficient strategy for neurostimulation.

In the present study, we demonstrate a selective brain stimulation method through manipulating the activity of a mechanosensitive ion channel, MscL-G22S, by non-invasive ultrasound both *in vitro* and *in vivo*. The MscL-G22S channel is a mutant version of the well-established bacterial large-conductance mechanosensitive channel. It has a lower threshold for gating than wild-type MscL but does not show spontaneous activity (Yoshimura et al., 1999) and has been shown to respond to ultrasound with microbubbles in retinal epithelia (Heureaux et al., 2014). We used this channel to sensitize 293T cells and primary neurons to ultrasound and used calcium (Ca^{2+}) imaging to detect Ca^{2+} influx upon ultrasonic stimulation. We found that ultrasound could consistently induce a Ca^{2+} influx into cells at significantly lower intensities in MscL-G22S-expressing cells compared with those that did not. We also used viruses with specific promoters to express MscL-G22S only in desired cell-types in the brain. Ultrasound stimulation of MscL-G22S-expressing excitatory neurons in mouse cortices evoked much stronger muscular responses in mouse limbs, as measured by electromyogram (EMG), and these responses were evoked at lowered intensities. MscL-expressing neurons in the cortex also showed significantly higher neuronal activation when stimulated with lower-intensity ultrasound compared with a control. Crucially, we also observed that expressing MscL-G22S in cortical neurons alone was not enough to increase their baseline-activation levels. Finally, we stimulated neurons with MscL-G22S in the right dorsomedial striatum (DMS) of mice and compared the induced activation in both right and left DMSs and the cortices directly above them. Significantly more MscL-expressing neurons in the right DMS were activated than those not expressing the channel, and no activation increase was seen in the other regions. We thus demonstrate a spatially specific and cell-specific method of stimulating neurons with low-intensity ultrasound by inducing the expression of a mechanosensitive ion channel.

RESULTS

Low-Intensity Ultrasound Can Stimulate Ca^{2+} Influx in 293T Cells Expressing MscL-G22S

For our study, we used a customized system combining ultrasound and calcium imaging as detailed in our previous study (Qiu et al., 2019). The ultrasound transducer was set up at a 45° angle to the cells to minimize the standing waves generated, and a strong water-air interface was created on the base of the culture dish, resulting in a controllable ultrasound field, as mapped by a hydrophone and a high-precision 3D motor. We also used ultrasound parameters aimed at achieving short bursts of ultrasound "On" times (300 ms stimulation duration) at a center frequency of 500 kHz and low intensities, at which no temperature elevation was observed (data not shown).

Our overall scheme was to introduce the mechanosensitive MscL-G22S into cells as a method of sensitizing cells to ultrasound and enabling increased Ca^{2+} influx (Figure 1A). We first confirmed that heterologously expressed MscL-G22S could sensitize cells to ultrasound in our system. We used 293T cells, known to have minimal endogenous expression of mechanosensitive ion channels (Coste et al., 2010; Syeda et al., 2015) and transfected a plasmid encoding a MscL-G22S-EGFP fusion protein (designed by Cox et al., 2016). Expression of MscL-G22S in 293T cells was verified by qPCR and fluorescence imaging compared with a mock transfection control (Figure 1B). We initially tested our ultrasound setup with a patch clamping system but found the giga-seal to be unstable because of ultrasound-induced vibration (data not shown). Thus, we instead used Ca^{2+} imaging with a ratiometric fluorescent calcium indicator (Fura-2) to observe and measure the movement of calcium ions into cells. Cells were treated with ultrasound at pressures from 0.025 to 0.15 MPa. Cells expressing MscL-G22S showed significantly greater Ca^{2+} influx in response to a single 300-ms ultrasound pulse than the control did, and that response was abrogated when MscL-expressing cells were imaged in Ca^{2+}-free solution (Figures 1C and 1D). Mock-transfected cells showed no response at any of the applied pressures, but MscL-expressing cells showed increased responses at greater intensities (Figure 1E). In addition to assessing the degree of Ca^{2+} response, the ratiometric nature of the Ca^{2+} dye used enabled us to ascertain that the increase in fluorescence seen was not an artifact of the ultrasound setup. We thus found that expressing MscL-G22S could successfully sensitize 293T cells to ultrasound stimulation at the low frequency of 500 kHz without the use of microbubbles.

Expressing MscL-G22S Significantly Reduces the Ultrasound Intensity Required to Provoke Ca^{2+} Influx in Mouse Primary Neurons

We next tested the effects of ultrasound on primary cortical neurons harvested from embryonic mouse brains (E16) to test the feasibility of selectively stimulating live neurons with ultrasound. To induce MscL-G22S expression in neurons, we used adeno-associated virus (AAV)-based viruses with a human synapsin (hSyn) promoter, which preferentially infects neurons over other cell types. We first confirmed the neuron specificity of our viruses by transducting primary neurons at 7 days *in vitro* (DIV 7) with rAAV/9-hSyn:MscL-G22S-EYFP-pA or rAAV/9-hSyn:EYFP-pA (empty vector) viruses. At DIV 12, transducted neurons were found to show enhanced yellow fluorescent protein (EYFP) co-located with the expression of the neuron marker MAP2 (Figure 2A), thus confirming the neuron specificity of the viruses. The resting membrane potential of neurons, measured by a current clamp, was not significantly different between the two groups, thus indicating that

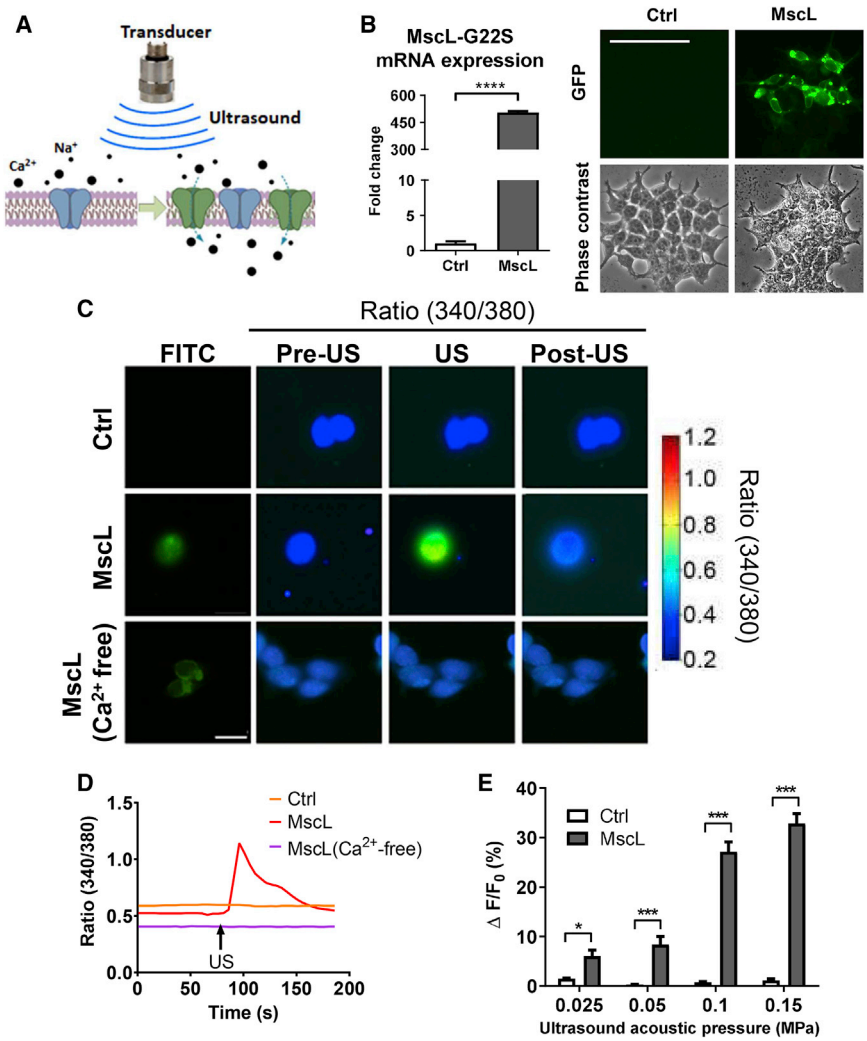

Figure 1. Low-Intensity Ultrasound Induces Ca^{2+} Influx into 293T Cells Expressing MscL-G22S

(A) Schematic representation of our approach. Briefly, this involves sensitizing cells to ultrasound by heterologously expressing a mechanosensitive ion channel, MscL-G22S, in their cell membranes. These channels should then react to ultrasound stimulation by opening, allowing the entry of cations such as Ca^{2+}.

(B) Expression of MscL-G22S in transfected cells ("MscL") was assessed by qRT-PCR and microscopy, in comparison with a mock-transfection control ("Ctrl") (normalized to β-actin). Left: the bar chart of qPCR results represents means ± SEM of three independent experiments, n = 3, ***p < 0.001. Right: representative images of GFP fluorescence and phase contrast are shown.

(C) Representative images of ratiometric Ca^{2+} imaging of Ctrl and MscL cells before, during, and after being stimulated by a single ultrasound pulse (0.15 MPa, 300 ms stimulation duration, 300 μs pulse width, 40% duty cycle, 500 kHz center frequency, 1 kHz PRF).

(D) A representative time course of ratiometric Ca^{2+} imaging comparing Ca^{2+} response upon ultrasound stimulation of Ctrl and MscL-transfected cells at 0.15 MPa for a single pulse, and the MscL cells' reaction when placed in a Ca^{2+}-free medium.

(E) Ca^{2+} response of cells to different ultrasound intensities. Bar chart represents means ± SEM of three independent Ca^{2+} imaging experiments. n = 9, *p < 0.05, ***p < 0.001, two-tailed unpaired t test with Holm-Sidak correction.

All scale bars in this figure represent 100 μm.

the general health and excitability of neurons was not affected by overexpressing MscL-G22S (Figure 2B). For Ca^{2+} imaging, primary neurons at DIV 7 were transducted with rAAV/9-hSyn:MscL-G22S::GCaMP6S or rAAV/9-hSyn::GCaMP6S, where GCaMP6S is a fluorescent calcium-indicator protein (Chen et al., 2013), and calcium imaging was performed at DIV 12. Neurons expressing MscL-G22S accumulated significantly more intracellular Ca^{2+} compared with the control in response to ultrasound (Figure 2C). Primary neurons expressing MscL-G22S-GCaMP6S showed quick and reversible Ca^{2+} response to each ultrasound stimulus, whereas those expressing GCaMP6S alone showed no significant response (Figure 2D). The neural response also showed some adaptation to the ultrasound stimulus, with the Ca^{2+} influx amplitude decreasing slightly upon repeated stimulation. MscL-G22S-expressing neurons showed dose-dependent Ca^{2+} influx response, with increasing acoustic pressure inducing greater Ca^{2+} influx (Figure 2E). At 0.05 MPa, these neurons showed significant Ca^{2+} influx, whereas the control showed little to no change. The control cells showed significantly lower Ca^{2+} influx than the MscL-G22S-expressing cells, up to 0.45 MPa, at which intensity other mechanosensitive elements of the cells appeared to come into play. We also compared the ultrasound responses of primary neurons plated on a 1 kPa of polyacrylamide gel, much softer than glass and close to the stiffness of the brain, transducted with these viruses. We again found that the MscL-G22S-expressing cells responded strongly and specifically to ultrasound stimuli, but the control cells did not (Figure S1), indicating that the cellular responses we observed from cells plated on glass were not significantly skewed because of the hard substrate. We thus found that introducing MscL-G22S into primary neurons did not alter their baseline excitability but successfully sensitized them to ultrasound, as reflected in the significantly lowered intensities at which neurons were able to respond to ultrasound.

Low-Intensity Ultrasound Evokes Muscular Responses and Activates Neurons with MscL-G22S

We tested the *in vivo* feasibility of our setup by stimulating mouse brains expressing MscL-G22S in different regions. rAAV/9-hSyn:MscL-G22S-EYFP-pA, pAOV/CaMKIIα:MscL-G22S-EYFP-3FLAG, or their respective empty control viruses

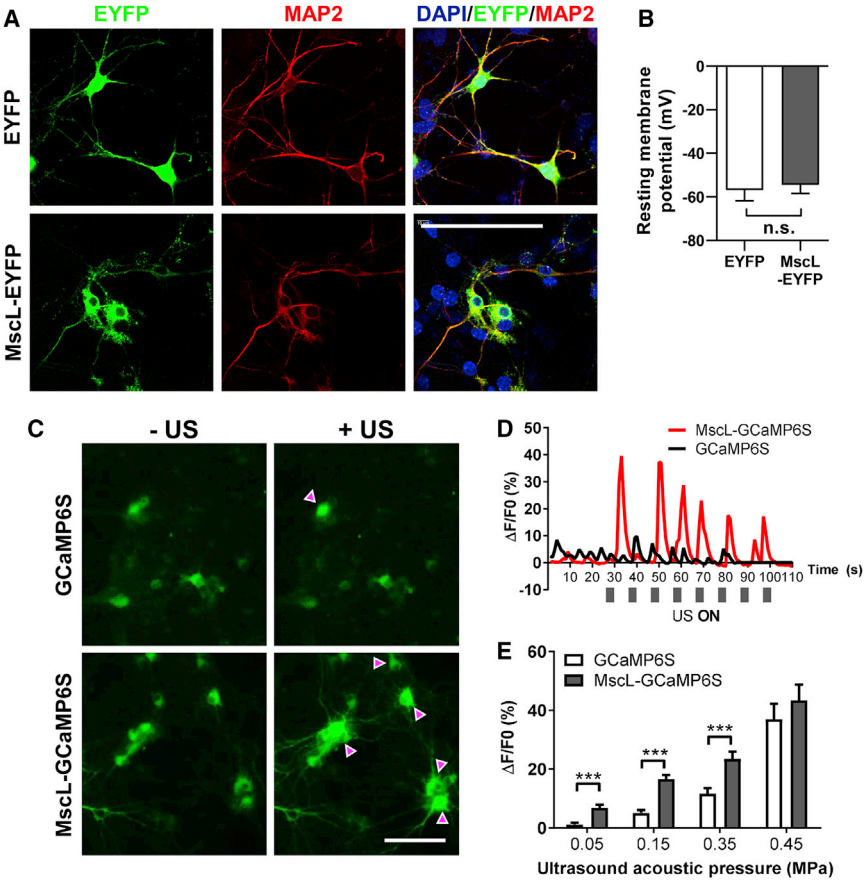

Figure 2. Mouse Primary Neurons Expressing MscL-G22S Show Significantly Increased Ca^{2+} Influx in Response to Low-Intensity Ultrasound

(A) Representative immunocytochemical staining of primary neurons transducted with rAAV/9-hSyn:EYFP-pA and rAAV/9-hSyn:MscL-G22S-EYFP-pA viruses at DIV 12. Cells were imaged for MAP2 (red) staining and EYFP fluorescence (green) to confirm the virus' ability to preferentially transduct neurons.

(B) Resting membrane potentials of individual neurons as measured by current clamping. The bar chart represents means ± SEM of measurements of individual neurons. n for Ctrl = 4, MscL = 6; results were compared using an unpaired two-tailed t test with Welch's correction.

(C) Representative Ca^{2+} imaging result of primary neurons transducted with rAAV/9-hSyn:GCaMP6S-pA and rAAV/9-hSyn:MscL-G22S-GCaMP6S-pA viruses, and stimulated with 0.15 MPa ultrasound at DIV 12.

(D) Representative Ca^{2+} imaging time-course of a single neuron each transducted with the respective viruses, and their responses to repeated ultrasound pulses (0.15 MPa, 300 ms stimulation duration, 300 μs pulse width, 40% duty cycle, 500 kHz center frequency, 1 kHz PRF).

(E) Ca^{2+} response of primary cortical neurons expressing GCaMP6S to different ultrasound intensities. The bar chart represents means ± SEM of neurons stimulated with ultrasound at varying intensities from three independent experiments. n = 25, ***p < 0.001, unpaired 2-tailed t tests with Holm-Sidak correction.

All scale bars in this figure represent 100 μm.

See also Figure S1.

were injected into the right cerebral cortices of 8-week-old mice. The injection site approximately corresponded to the primary motor cortex region (M1). We first tested whether we could sensitize neurons in the brain enough to evoke a simple twitch response. For this, we used CaMKIIα-promoted MscL-G22S/control viruses, which allowed us cell-type specificity by targeting only excitatory neurons. Four weeks after injection, mice were anesthetized, a mounted transducer setup was aligned to the transducted cortical region, and an EMG probe was attached to the triceps muscles in the left forelimb (Figure 3A). We found that stimulation of MscL-expressing brains at low intensities could evoke sonication-evoked contractions, with little-to-no response in the control condition (Figure 3B). Both the magnitude of response (relative amplitude) and the rate of response were greater in MscL-G22S mice, and a general pattern of dose dependence was observed (Figures 3C and 3D). At the lower acoustic intensities of 0.005 and 0.15 MPa, we observed no EMG response in the control (EYFP only) mice, with minor responses at higher acoustic pressures; however, MscL-G22S mice showed distinct responses at all tested intensities. The EMG response latency was stable between the two mice at approximately 150 ms, showing no significant differences because of the viruses and was comparable to previous findings *in vivo* (King et al., 2013). Thus, MscL-G22S expression could successfully sensitize excitatory neurons to ultrasound stimulation, resulting in increased EMG response amplitude and success rate with a temporal resolution within 200 ms of stimulation.

We then studied the effect of MscL-G22S expression in the M1 region upon the ability of ultrasound stimuli to activate neurons in the brain. Five weeks after injection, mice expressing hSyn-promoted viruses were subjected to 0.3 MPa ultrasound stimulation for 40 min under anesthesia (Figure 4A). The regions of viral expression were located by EYFP fluorescence, and neuronal activation in the mice subjects was evaluated by staining for the important activation marker c-Fos, which is known to depend on calcium influx (Ghosh et al., 1994; Sheng and Greenberg, 1990). c-Fos expression was seen to be upregulated only within the region of the EYFP expression in the MscL-expressing mouse cortices (Figure 4B). Ultrasound treatment induced greater expression of c-Fos in the nuclei of MscL-expressing cortical neurons compared with the control cortices stimulated with ultrasound and both non-ultrasound conditions (Figure 4C). $c\text{-}Fos^{+}$ cells in MscL-expressing ultrasound-stimulated cells were more than double the number in control cortices and four times that in non-stimulated MscL-expressing cells, showing the specificity of our strategy combining ultrasound and sensitization by mechanosensitive ion channel expression (Figure 4D). A small increase in c-Fos expression was observed in the control

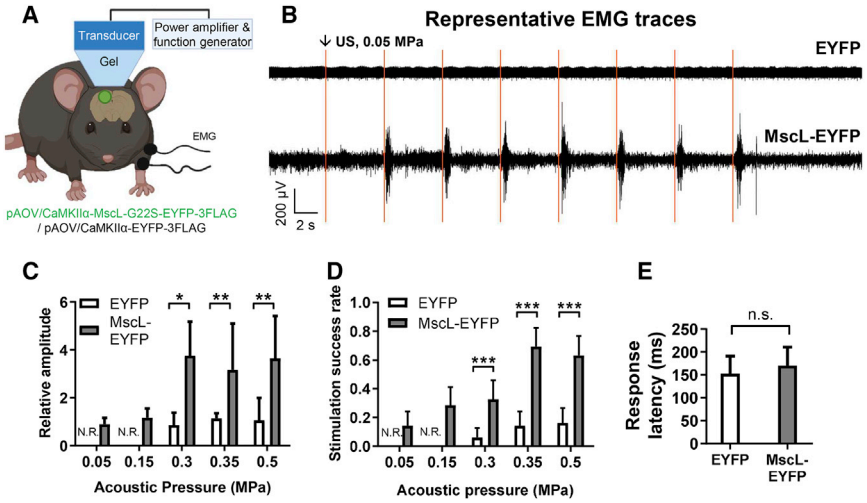

Figure 3. Ultrasound Stimulation Evokes Greater Muscular Responses When Applied to Mouse Cortices Expressing MscL-G22S

(A) Schematic illustration of our *in vivo* neuron sensitization and ultrasound stimulation plan. Briefly, mice at 8 weeks were injected with CaMKIIα-promoted viruses in their right cerebral cortices; 4 weeks later, anesthetized mice were treated with ultrasound and muscular response in the triceps of the left forelimb was recorded using an EMG probe.

(B) Representative EMG traces of muscular responses upon ultrasound stimulation in mice expressing the control or MscL-G22S viruses pulse (0.05 MPa, 300 ms stimulation duration, 400 μs pulse width, 40% duty cycle, 500 kHz center frequency, 1 kHz PRF).

(C) Relative amplitude (peak identified signal/signal baseline) of EMG response upon stimulation by ultrasound of varying intensities. N.R., no response, measured according to the stated data-processing method. Data represent means ± SD, n = 49.

(D) Success rate of each delivered ultrasound stimulus to evoke EMG spikes (peak identified signal/signal baseline) of EMG response upon stimulation by ultrasound of varying intensities. N.R., no response, measured according to the stated data-processing method. Data represent means ± SD, n = 7, except for CaMKII-EYFP, n = 3.

(E) Latency between ultrasound stimulus and above-threshold response detection. Data represent means ± SD, n = 6.

Statistical significance for (C), (D), and (E) was determined by an unpaired two-tailed t test with Holm-Sidak correction. *p < 0.05, **p < 0.01, ***p < 0.001.

cells treated with ultrasound, around three times that of unstimulated cells, but that difference was not statistically significant. A similar comparison of mice with sham injections showed no significant difference in c-Fos expression between the cortices of mice treated or untreated with ultrasound (Figure S2A), and the groups showed no obvious health differences as judged by body weight (Figure S2B). We thus found that the application of ultrasound to mouse cortices could induce some neuronal activity, but the induced MscL expression made that effect many times stronger. Furthermore, the spatial extent of neural activation was largely co-located with MscL expression in the cortex. We also found that making neurons *in vivo* express MscL-G22S did not alter their resting membrane potentials compared with the control virus, as measured by current clamping of neurons from acute brain slices (Figure 4E). Therefore, expressing MscL-G22S in the cortices of mouse brains could successfully sensitize neurons to activation by ultrasound.

MscL-G22S Expression Enables Targeted Neurostimulation in the DMS Region by Low-Intensity Ultrasound

We tested the spatial selectivity of our ultrasound stimulation method, by using the MscL-G22S virus to sensitize neurons in a deeper region of the brain. hSyn-promoted MscL-G22S-EYFP or its corresponding control virus was injected into the right DMS of 6-week-old mice. Five weeks later, those mice were subjected to 0.3 MPa of ultrasound stimulation for 40 min under anesthesia using a mounted transducer setup (Figure 5A). These brains were then evaluated for nuclear c-Fos expression in the right DMS injected with virus, the cortical region directly above the right DMS, and both contralateral regions. The right DMS region expressing MscL-G22S in its neurons showed significantly greater neuronal activation than all other groups (Figures 5B and 5C). A small but statistically insignificant increase was seen in the control cells stimulated with ultrasound, but this was much less than in the MscL-G22S cells (mean, 51.85 c-Fos$^+$ cells/slice in the control versus 93.12 in the MscL-G22S condition), indicating MscL's ability to efficiently sensitize cells to ultrasound stimulation. No significant changes in c-Fos expression were observed in either of the contralateral sides or in the cortical regions above the DMS. We also investigated the c-Fos levels in the same brain regions of the mice that had received the virus but were not treated with ultrasound. No significant changes were found in the DMS and the cortices of those mice (Figure S2C). Finally, no significant differences were seen between groups with sham viral injection (Figure S2D). Therefore, using our setup, we were able to selectively activate neurons in the right DMS regions of mice, sensitized through the expression of MscL-G22S, without any concurrent activation of neurons in the nearby cortex or in either contralateral region. Even in neurons that may be more inherently mechanosensitive, such as those in the DMS, compared with those in the cortex, MscL expression could significantly increase their sensitivity to ultrasound. Furthermore, the increased neuronal activation was observed primarily in brain regions targeted using MscL-G22S expression, indicating that the effects observed were due to ultrasound and not to unintended widespread auditory effects. Finally, the experiment also confirmed the ability of ultrasound generated by our setup to penetrate regions of the brain deeper than the cortex, making it suitable for *in vivo* use in areas of the brain both relatively superficial and deep.

DISCUSSION

The present study demonstrates a mechanosensitive ion-channel-mediated, spatially specific ultrasound-neurostimulation strategy in the brains of mice. We were able to induce neuron-specific activity in both primary neurons as well as in the right

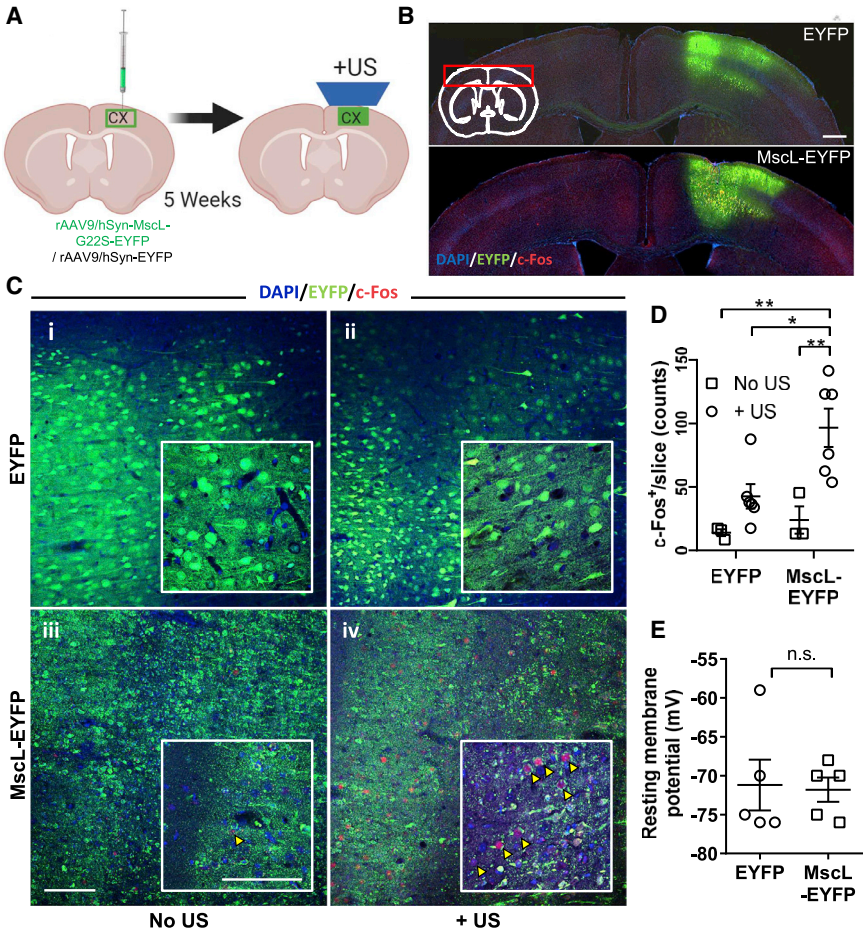

Figure 4. Low-Intensity Ultrasound Activates Significantly More Neurons in Mouse Cerebral Cortices Expressing MscL-G22S

(A) Schematic illustration of our *in vivo* neuron sensitization and ultrasound stimulation plan. Briefly, mice at 8 weeks were injected with viruses in their cerebral cortices, and 5 weeks later, they were treated with 0.3 MPa ultrasound for a 40-min pulse (300 ms stimulation duration, 400 μs pulse width, 40% duty cycle, 500 kHz center frequency, 1 kHz PRF). The mice were sacrificed after an interval of 90 min, and their brains were imaged for DAPI, EYFP, and c-Fos expression. Scale bar represents 500 μm.

(B) Low magnification of mouse brains expressing hSyn:MscL-EYFP or hSyn:EYFP, showing the areas of EYFP and c-Fos expression in the cerebral cortex. Scale bar in this panel represents 50 μm.

(C) Representative images of mouse cortices treated with or without ultrasound, stained for c-Fos expression. All scale bars in this panel represent 100 μm.

(D) Counts of nuclear c-Fos per slice imaged. The bar chart represents means ± SEM of c-Fos$^+$ cells per stained slice. *n* for + ultrasound (US) groups = 6 and for No-US groups = 3. *p < 0.05, **p < 0.01, two-way ANOVA with post hoc Tukey test. All significant differences are indicated in the graph.

(E) Resting membrane potentials of virus-transducted neurons from acute brain slices of cerebral cortices. The bar chart represents means ± SEM of measurements taken from different mice, n = 5. Results were compared using an unpaired two-tailed t test with Welch's correction.

See also Figure S2.

cortex and DMS of mice, using ultrasound applied non-invasively without observing effects in other brain regions. We observed low or no EMG response from cells not expressing MscL-G22S but clear and significantly greater response from MscL-expressing cells when stimulated with ultrasound. Crucially, upon ultrasound stimulation of the right DMS, located deeper than the cortex, we did not detect increased activation of neurons in either the ipsilateral or contralateral cortices. Neuronal activation was restricted to the respective cortex or DMS that both expressed MscL-G22S and was stimulated by ultrasound. When MscL-expressing neurons in the DMS were treated with ultrasound, we did not find increased c-Fos levels either in the cortical area above it or the contralateral cortex. This helps to establish that the activation of neurons observed was due to the ultrasound treatment and not to the generalized cortical activation through the auditory pathway observed in other studies (Guo et al., 2018; Sato et al., 2018). Studies performed by other groups have also stressed ultrasound as directly activating neurons without significant confounding from auditory pathways (Mohammadjavadi et al., 2019; Niu et al., 2018). The non-invasiveness and penetrative reach of this approach are promising for eventual clinical translation, whereas the cell-type selectivity could facilitate the elucidation and management of neural circuits involved in specific behaviors or disorders. Such a combination of these two features would be immensely helpful to target areas in the deep brain in conditions in which treatments require non-invasiveness and repeatability e.g., targeting the *substantia nigra* in Parkinson's disease. Furthermore, the spatial specificity of neural activation targeted by MscL-G22S could be further fine-tuned by using focused ultrasound, which is compatible with other imaging modalities, such as MRI, to achieve dynamic and precise focus in desired regions.

We found that increasing acoustic pressure above certain points in our study evoked responses in non-MscL-expressing cells or tissues as well, suggesting some inherent level of mechanosensitivity in the brain, which we have detailed elsewhere (Qiu et al., 2019). These findings stress the importance of understanding the inherent mechanosensitive properties of the brain and its various regions and of neurons, which are now widely understood to have some ability to sense physical forces (Tyler, 2012). At the lower end of ultrasound pressures applied, we found that MscL-G22S-expressing cells were able to respond to ultrasound with minimal response in the control group. Hence, keeping the ultrasound intensity low could be a way of limiting the ultrasound effects to only the desired cell types and the desired area. Such specificity is crucial in the eventual

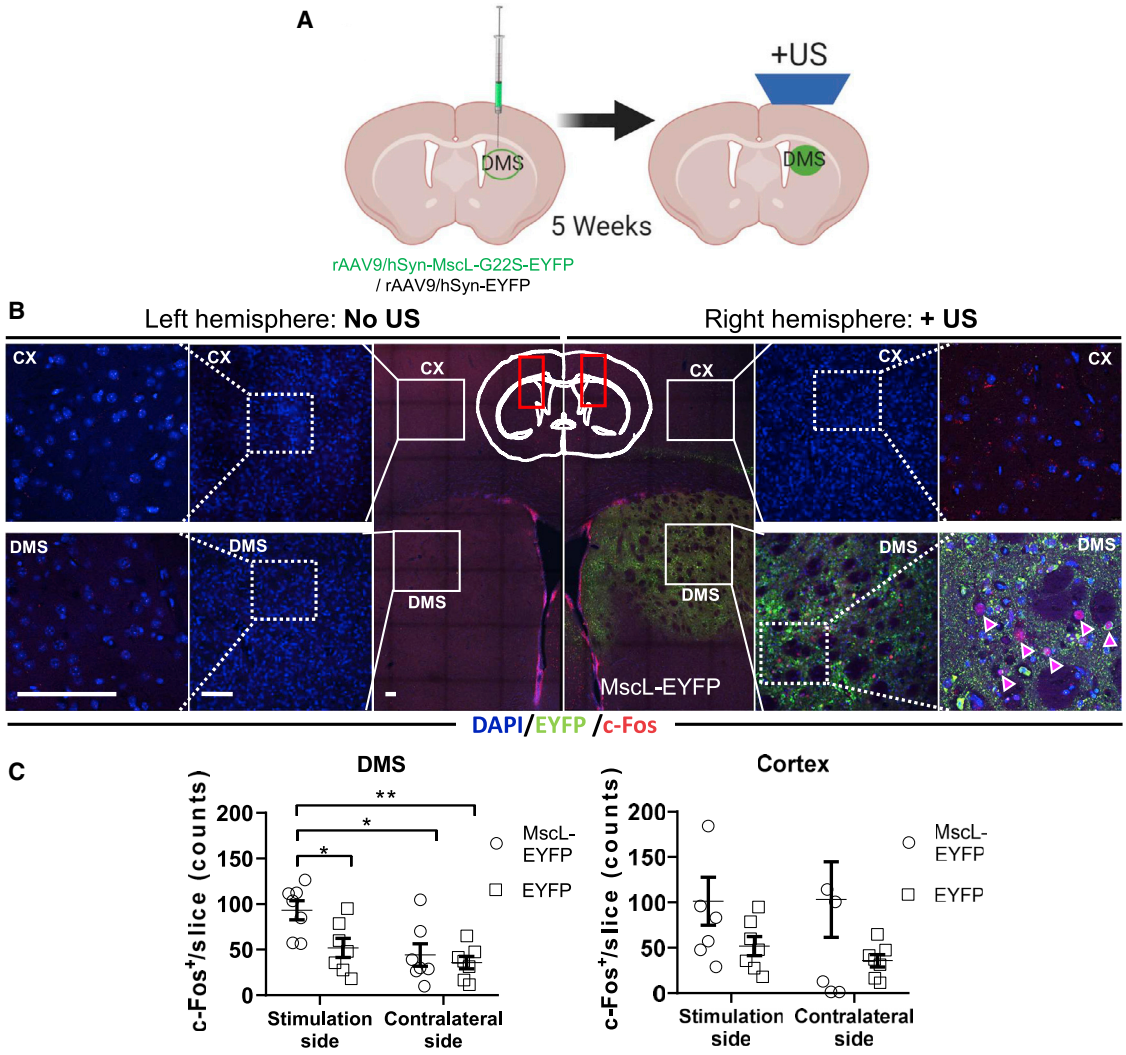

Figure 5. Neuronal Activation by Targeted Low-Intensity Ultrasound Is Localized to the Brain Region Expressing MscL-G22S

(A) Schematic illustration of our *in vivo* neuron sensitization and ultrasound stimulation plan. Briefly, mice at 6 weeks were injected with hSyn:MscL-G22S-EYFP in their right dorsomedial striatum (DMS), and 5 weeks later, they were treated with 0.3 MPa ultrasound for a 40-min pulse (300 ms stimulation duration, 400 μs pulse width, 40% duty cycle, 500 kHz center frequency, 1 kHz PRF). The mice were sacrificed after an interval of 90 min, and their brains were imaged for DAPI, EYFP, and c-Fos expression.

(B) Representative images of the left and right DMS and the regions of cerebral cortex directly above it, expressing DAPI, EYFP, and c-Fos. All scale bars in this panel represent 100 μm.

(C) Counts of nuclear c-Fos per slice imaged in the DMS and cortices of mice treated with ultrasound. The bar chart represents means ± SEM of c-Fos$^+$ cells per stained slice. n = 6. *p < 0.05, **p < 0.01, two-way ANOVA with post hoc Tukey test. All significant differences are indicated.

See also Figure S2.

development of ultrasound-based treatments and could be useful in minimizing side effects.

EMG responses showed that the temporal resolution of our approach is within 200 ms, and Ca^{2+} imaging and c-Fos activation provide cell-level evidence of targeted neural activation *in vitro* and *in vivo*. The major limitation of this study is that it lacks information about ion-channel dynamics, which could be obtained by patch clamping during ultrasound stimulation. We were unfortunately unable to do this because of background vibration encountered in the patch pipettes during sonication, an observation consistent with previous studies (Prieto et al., 2018; Tyler et al., 2008). We were thus restricted to observing the activity of Ca^{2+} influx using Ca^{2+} imaging, which is inferior at tracking temporal dynamics than patch clamping. Whether low-frequency ultrasound alone can directly activate mechanosensitive ion channels by acting on them directly or on some other mechanism is, therefore, an issue that requires deeper elucidation. Developing patch clamping methods compatible with low-frequency ultrasound would enable us to ascertain the temporal resolution and temporal profile of ultrasound's

effects on ion channels. It would also help to identify the lower limits of intensities required for successful stimulation, thereby helping to further reduce unintended activation and side effects through mechanistic insights. Real-time monitoring of cellular responses would also be immensely valuable for *in vivo* data because it could further help to identify cellular responses to ultrasound more specifically and eliminate problems such as the possible auditory confound. Such monitoring could also differentially measure the responses from the cell types in the brain other than neurons. Future *in vivo* studies could, hence, use one of a few approaches, such as genetically encoded Ca^{2+} indicators and voltage sensors, neurotransmitter sensors, or cellular recording methods, such as electrocorticography (ECoG), to gauge the effectiveness of ultrasound stimulation and to provide depth to behavioral studies.

During the experiments detailed in the present study, we did not observe obvious side effects of MscL-G22S expression as indicated by mouse behavior and body weight, resting membrane potential of primary neurons, etc. However, more-detailed experiments are needed to test the possible artifacts of such a treatment. The G22S mutant of MscL is reported not to be spontaneously active (Yoshimura et al., 1999), which could plausibly explain the lack of these indicators; nevertheless, it remains crucial to reduce the possibility of adverse effects as much as possible. Nevertheless, we observed a minor increase in nuclear c-Fos in DMS neurons expressing MscL-G22S, indicating that some background effects of introducing such an ion channel might be unavoidable. MscL is a non-selective ion channel and has a large pore size (larger than 30 Å, according to Cruickshank and colleagues [Cruickshank et al., 1997]). Therefore, it conducts ions other than Ca^{2+} and even small proteins, which could further complicate the profile of activation effects, and it will require specific experiments to tease out the effects of individual factors from the others.

The performance of this approach can be further improved by using other ultrasonic-sensitive ion channels or engineering novel MscL mutants. On the other hand, mechanosensitive potassium or chloride channels may also serve as potential mediators with inhibitory effects, making it possible to reduce neural activity as well (Wietek et al., 2015). Moreover, the ultrasonic paradigm may be expanded to trigger mechanosensitive ion channels endogenously expressed in various tissues, such as the peripheral or enteric nervous system, which could have therapeutic implications. Such non-invasive control of neurons in deep tissue, whether in the brain or elsewhere, whose inaccessibility currently poses substantial challenges to biomedicine could be a way to address diseases and neurological conditions of many varieties in the future.

Although the experiments detailed in the present study involve a minimally invasive procedure to induce the expression of MscL-G22S, the availability of newer methods could potentially eliminate that need. Recently, the novel rAAV/PHP.eB, which can infect neurons in the brain through a simple tail-vein injection (Chan et al., 2017), showed potentially noninvasive gene delivery to specific neurons. With further development, such technology could reduce the severity of the invasion even further, thus making it easier to implement a system like ours.

STAR★METHODS

Detailed methods are provided in the online version of this paper and include the following:

- KEY RESOURCES TABLE
- RESOURCE AVAILABILITY
  - Lead Contact
  - Materials Availability
  - Data and Code Availability
- EXPERIMENTAL MODEL AND SUBJECT DETAILS
  - Animals
  - Cell lines and primary cultures
- METHOD DETAILS
  - Plasmid transfection
  - Preparation of PA hydrogels for neuron culture
  - Viruses
  - Viral transduction
  - *In vitro* ultrasound stimulation system and protocol
  - Patch clamp
  - Calcium imaging
  - RNA extraction and reverse-transcription
  - Real-time qPCR
  - Immunocytochemical fluorescent staining
  - Stereotaxic injection
  - EMG recording in anesthetized mice and data processing
  - Ultrasound stimulation in cortex and DMS
  - Immunohistochemical fluorescent staining
  - Electrophysiology of acute brain slices
- QUANTIFICATION AND STATISTICAL ANALYSIS

SUPPLEMENTAL INFORMATION

Supplemental Information can be found online at https://doi.org/10.1016/j.celrep.2020.108033.

ACKNOWLEDGMENTS

We thank Dr. Boris Martinac for the generous provision of the MscL-G22S plasmid. This work was supported by Key-Area Research and Development Program of Guangdong Province (2018B030331001), the Hong Kong Research Grants Council General Research Fund (15102417 and 15326416), Hong Kong Innovation Technology Fund Mid-stream Research Program (MRP/018/18X), Shenzhen Science and Technology Innovation Commission Basic Research Program (JCYJ20160531184809079), and internal funding from the Hong Kong Polytechnic University (1-ZE1K and 1-BBAU).

AUTHOR CONTRIBUTIONS

Conceptualization, Z.Q. and L.S; Methodology, S.K., J.G., Z.Q., and L.S.; Investigation, S.K., J.G., Z.Q., Q.X., J.Z., X.H., T.Z., M.Y., H.W., and K.F.W.; Formal Analysis, Z.Q., S.K., Q.X., and K.F.W.; Writing—Original Draft, Q.Z., S.K., J.G., Q.X., and L.S.; Writing—Review and Editing, Z.Q., S.K., J.G., Q.X., J.Z., K.F.W., and L.S.; Supervision, J.G. and L.S.; Funding Acquisition, L.S.

DECLARATION OF INTERESTS

The authors have submitted a patent application titled "A non-invasive method for selective neural stimulation by ultrasound" with the U.S. Patent and Trade Office, dated April 10, 2018, assigned application number 15/949,991.

Received: June 28, 2019
Revised: September 11, 2019
Accepted: July 23, 2020
Published: August 18, 2020

REFERENCES

Anderson, D.J. (2012). Optogenetics, sex, and violence in the brain: implications for psychiatry. Biol. Psychiatry *71*, 1081–1089.

Bystritsky, A., and Korb, A.S. (2015). A review of low-intensity transcranial focused ultrasound for clinical applications. Curr. Behav. Neurosci. Rep. *2*, 60–66.

Chan, K.Y., Jang, M.J., Yoo, B.B., Greenbaum, A., Ravi, N., Wu, W.L., Sánchez-Guardado, L., Lois, C., Mazmanian, S.K., Deverman, B.E., and Gradinaru, V. (2017). Engineered AAVs for efficient noninvasive gene delivery to the central and peripheral nervous systems. Nat. Neurosci. *20*, 1172–1179.

Chen, T.W., Wardill, T.J., Sun, Y., Pulver, S.R., Renninger, S.L., Baohan, A., Schreiter, E.R., Kerr, R.A., Orger, M.B., Jayaraman, V., et al. (2013). Ultrasensitive fluorescent proteins for imaging neuronal activity. Nature *499*, 295–300.

Coste, B., Mathur, J., Schmidt, M., Earley, T.J., Ranade, S., Petrus, M.J., Dubin, A.E., and Patapoutian, A. (2010). Piezo1 and Piezo2 are essential components of distinct mechanically activated cation channels. Science *330*, 55–60.

Cox, C.D., Bae, C., Ziegler, L., Hartley, S., Nikolova-Krstevski, V., Rohde, P.R., Ng, C.A., Sachs, F., Gottlieb, P.A., and Martinac, B. (2016). Removal of the mechanoprotective influence of the cytoskeleton reveals PIEZO1 is gated by bilayer tension. Nat. Commun. *7*, 10366.

Cruickshank, C., Minchin, R.F., LeDain, A.C., and Martinac, B. (1997). Estimation of the pore size of the large-conductance mechanosensitive ion channel of *Escherichia coli*. Biophys. J. *73*, 1925–1931.

Ghosh, A., Ginty, D.D., Bading, H., and Greenberg, M.E. (1994). Calcium regulation of gene expression in neuronal cells. J. Neurobiol. *25*, 294–303.

Gomez, J.L., Bonaventura, J., Lesniak, W., Mathews, W.B., Sysa-Shah, P., Rodriguez, L.A., Ellis, R.J., Richie, C.T., Harvey, B.K., Dannals, R.F., et al. (2017). Chemogenetics revealed: DREADD occupancy and activation via converted clozapine. Science *357*, 503–507.

Guo, H., Hamilton, M., 2nd, Offutt, S.J., Gloeckner, C.D., Li, T., Kim, Y., Legon, W., Alford, J.K., and Lim, H.H. (2018). Ultrasound produces extensive brain activation via a cochlear pathway. Neuron *98*, 1020–1030.e4.

Heureaux, J., Chen, D., Murray, V.L., Deng, C.X., and Liu, A.P. (2014). Activation of a bacterial mechanosensitive channel in mammalian cells by cytoskeletal stress. Cell. Mol. Bioeng. *7*, 307–319.

Ibsen, S., Tong, A., Schutt, C., Esener, S., and Chalasani, S.H. (2015). Sonogenetics is a non-invasive approach to activating neurons in *Caenorhabditis elegans*. Nat. Commun. *6*, 8264.

Insel, T.R., Landis, S.C., and Collins, F.S.; The NIH BRAIN Initiative (2013). Research priorities. Science *340*, 687–688.

King, R.L., Brown, J.R., Newsome, W.T., and Pauly, K.B. (2013). Effective parameters for ultrasound-induced in vivo neurostimulation. Ultrasound Med. Biol. *39*, 312–331.

Kubanek, J., Shi, J., Marsh, J., Chen, D., Deng, C., and Cui, J. (2016). Ultrasound modulates ion channel currents. Sci. Rep. *6*, 24170.

Lang, N., Nitsche, M.A., Paulus, W., Rothwell, J.C., and Lemon, R.N. (2004). Effects of transcranial direct current stimulation over the human motor cortex on corticospinal and transcallosal excitability. Exp. Brain Res. *156*, 439–443.

Legon, W., Sato, T.F., Opitz, A., Mueller, J., Barbour, A., Williams, A., and Tyler, W.J. (2014). Transcranial focused ultrasound modulates the activity of primary somatosensory cortex in humans. Nat. Neurosci. *17*, 322–329.

Leinenga, G., Langton, C., Nisbet, R., and Götz, J. (2016). Ultrasound treatment of neurological diseases–current and emerging applications. Nat. Rev. Neurol. *12*, 161–174.

Lozano, A.M. (2017). Waving hello to noninvasive deep-brain stimulation. N. Engl. J. Med. *377*, 1096–1098.

Martinac, B. (2012). Mechanosensitive ion channels: an evolutionary and scientific tour de force in mechanobiology. Channels (Austin) *6*, 211–213.

Mohammadjavadi, M., Ye, P.P., Xia, A., Brown, J., Popelka, G., and Pauly, K.B. (2019). Elimination of peripheral auditory pathway activation does not affect motor responses from ultrasound neuromodulation. Brain Stimul. *12*, 901–910.

Nitsche, M.A., and Paulus, W. (2000). Excitability changes induced in the human motor cortex by weak transcranial direct current stimulation. J. Physiol. *527*, 633–639.

Niu, X., Yu, K., and He, B. (2018). On the neuromodulatory pathways of the in vivo brain by means of transcranial focused ultrasound. Curr. Opin. Biomed. Eng. *8*, 61–69.

Okun, M.S. (2014). Deep-brain stimulation—entering the era of human neural-network modulation. N. Engl. J. Med. *371*, 1369–1373.

Pan, Y., Yoon, S., Sun, J., Huang, Z., Lee, C., Allen, M., Wu, Y., Chang, Y.J., Sadelain, M., Shung, K.K., et al. (2018). Mechanogenetics for the remote and noninvasive control of cancer immunotherapy. Proc. Natl. Acad. Sci. USA *115*, 992–997.

Pi, R., Li, W., Lee, N.T., Chan, H.H., Pu, Y., Chan, L.N., Sucher, N.J., Chang, D.C., Li, M., and Han, Y. (2004). Minocycline prevents glutamate-induced apoptosis of cerebellar granule neurons by differential regulation of p38 and Akt pathways. J. Neurochem. *91*, 1219–1230.

Prieto, M.L., Firouzi, K., Khuri-Yakub, B.T., and Maduke, M. (2018). Activation of Piezo1 but Not $Na_V1.2$ channels by ultrasound at 43 MHz. Ultrasound Med. Biol. *44*, 1217–1232.

Qiu, Z., Guo, J., Kala, S., Zhu, J., Xian, Q., Qiu, W., Li, G., Zhu, T., Meng, L., Zhang, R., et al. (2019). The mechanosensitive ion channel piezo1 significantly mediates in vitro ultrasonic stimulation of neurons. iScience *21*, 448–457.

Rajasethupathy, P., Ferenczi, E., and Deisseroth, K. (2016). Targeting neural circuits. Cell *165*, 524–534.

Roy, D.S., Arons, A., Mitchell, T.I., Pignatelli, M., Ryan, T.J., and Tonegawa, S. (2016). Memory retrieval by activating engram cells in mouse models of early Alzheimer's disease. Nature *531*, 508–512.

Sato, T., Shapiro, M.G., and Tsao, D.Y. (2018). Ultrasonic neuromodulation causes widespread cortical activation via an indirect auditory mechanism. Neuron *98*, 1031–1041.e5.

Sheng, M., and Greenberg, M.E. (1990). The regulation and function of c-fos and other immediate early genes in the nervous system. Neuron *4*, 477–485.

Syeda, R., Xu, J., Dubin, A.E., Coste, B., Mathur, J., Huynh, T., Matzen, J., Lao, J., Tully, D.C., Engels, I.H., et al. (2015). Chemical activation of the mechanotransduction channel Piezo1. eLife *4*, e07369.

Tse, J.R., and Engler, A.J. (2010). Preparation of hydrogel substrates with tunable mechanical properties. Curr. Protoc. Cell. Biol. *Chapter 10*, Unit 10.16.

Tufail, Y., Matyushov, A., Baldwin, N., Tauchmann, M.L., Georges, J., Yoshihiro, A., Tillery, S.I., and Tyler, W.J. (2010). Transcranial pulsed ultrasound stimulates intact brain circuits. Neuron *66*, 681–694.

Tyler, W.J. (2012). The mechanobiology of brain function. Nat. Rev. Neurosci. *13*, 867–878.

Tyler, W.J., Tufail, Y., Finsterwald, M., Tauchmann, M.L., Olson, E.J., and Majestic, C. (2008). Remote excitation of neuronal circuits using low-intensity, low-frequency ultrasound. PLoS One *3*, e3511.

Tyler, W.J., Lani, S.W., and Hwang, G.M. (2018). Ultrasonic modulation of neural circuit activity. Curr. Opin. Neurobiol. *50*, 222–231.

Wietek, J., Beltramo, R., Scanziani, M., Hegemann, P., Oertner, T.G., and Wiegert, J.S. (2015). An improved chloride-conducting channelrhodopsin for light-induced inhibition of neuronal activity in vivo. Sci. Rep. *5*, 14807.

Ye, J., Tang, S., Meng, L., Li, X., Wen, X., Chen, S., Niu, L., Li, X., Qiu, W., Hu, H., et al. (2018). Ultrasonic control of neural activity through activation of the mechanosensitive channel MscL. Nano Lett. *18*, 4148–4155.

Yoshimura, K., Batiza, A., Schroeder, M., Blount, P., and Kung, C. (1999). Hydrophilicity of a single residue within MscL correlates with increased channel mechanosensitivity. Biophys. J. *77*, 1960–1972.

STAR★METHODS

KEY RESOURCES TABLE

REAGENT or RESOURCE	SOURCE	IDENTIFIER
Antibodies		
MAP2 polyclonal primary antibody	Invitrogen	Cat. # PA1-10005; RRID: AB_1076848
Goat anti-chicken IgY (H+L) Alexa Fluor 633	Invitrogen	Cat. # A-21103; RRID: AB_2535756
c-Fos (9F6) monoclonal primary antibody	Cell Signaling Technology	Cat. # 2250; RRID: AB_2247211
Goat anti-rabbit IgG (H+L), Alexa Fluor 555	Invitrogen	Cat. # A-21428; RRID: AB_2535849
Prolong Glass Antifade Mountant with NucBlue	Invitrogen	Cat. # P36981
Prolong Diamond Antifade Mountant with DAPI	Invitrogen	Cat. # P36971
Bacterial and Virus Strains		
rAAV/9-hSyn:EYFP-WPRE-pA	BrainVTA (Wuhan) Co. Ltd	Cat. # PT-0102
rAAV/9-hSyn:MscL-G22S-F2A-EYFP-WPRE-pA	BrainVTA (Wuhan) Co. Ltd	Cat. # PT-0280
rAAV/9-hSyn:MscL-G22S-2a-GCaMP6S-WPRE-pA	BrainVTA (Wuhan) Co. Ltd	Cat. # PT-0439
rAAV/9-hSyn:GCaMP6S-WPRE-pA	BrainVTA (Wuhan) Co. Ltd	Cat. # PT-0145
pAOV/CaMKIIa-EYFP-3FLAG	OBiO Technology, Shanghai	Cat. # AOV016
pAOV/CaMKIIa-MscL-G22S-EYFP-3FLAG	OBiO Technology, Shanghai	Cat. # H15130
Chemicals, Peptides, and Recombinant Proteins		
X-Rhodamine AM	Invitrogen	Cat. # X-14210
Fura-2 AM	Invitrogen	Cat. # F-1221
Experimental Models: Cell Lines		
Human: HEK293T cells	ATCC	Cat# CRL-3216, RRID: CVCL_0063
Experimental Models: Organisms/Strains		
Mouse: C57BL/6J	The Jackson Laboratory	JAX: 000664
Oligonucleotides		
Primer: Mouse β-actin: F - AGGGTGTGATGGTGGGAATG	Qiu et al., 2019	N/A
Primer: Mouse β-actin: R - TGGCGTGAGGGAGAGCATAG	Qiu et al., 2019	N/A
Primer: human β-actin: F - GTGGGGCGCCCCAGGCACCA	Qiu et al., 2019	N/A
Primer: human β-actin: R - CTCCTTAATGTCACGCACGATTTC	Qiu et al., 2019	N/A
Primer: MscL-G22S: F – GTCTCTTCACTGGTTGCCGA	This paper	N/A
Primer: MscL-G22S: R – TGCATCACAACAGCAGGGAT	This paper	N/A
Recombinant DNA		
pTRE-Tight MscL–T–eGFP	Martinac, 2012; Cox et al., 2016	
Software and Algorithms		
ImageJ		https://imagej.nih.gov/ij
GraphPad Prism 8.0	GraphPad Software, CA, USA	https://www.graphpad.com
MATLAB	The MathWorks, Inc., MA, USA	https://www.mathworks.com/products/matlab.html

RESOURCE AVAILABILITY

Lead Contact

Further information and request for reagents and resources should be addressed to, and will be fulfilled by, the Lead Contact, Lei Sun (lei.sun@polyu.edu.hk).

Materials Availability

This study did not generate new unique reagents.

Data and Code Availability

This study did not generate datasets.

EXPERIMENTAL MODEL AND SUBJECT DETAILS

Animals

Male, 8-week old, C57BL/6J mice, were used for cortical ultrasound stimulation. Female, 6-week old, C57BL/6J mice, were used for dorsomedial striatum (DMS) ultrasound stimulation. Mice were housed under standard housing condition with food and water available *ad libitum*. Animals from the abovementioned groups were assigned randomly to treatment groups. Animal use and care were performed following the guidelines of the Department of Health - Animals (Control of Experiments) of the Hong Kong S.A.R. government.

Cell lines and primary cultures

All cells were maintained inside a humidified incubator at 37°C with 5% CO_2. Human embryonic kidney 293T cells (referred to as '293T') were purchased from ATCC and were maintained in Dulbecco's Modified Eagle Medium (DMEM) (high glucose and no sodium pyruvate), supplemented with 10% fetal bovine serum, 100 units/mL penicillin and 100 μg/mL streptomycin (all from GIBCO),.

Primary cultures of mouse embryonic cortices at embryonic day 16 were obtained as previously described (Pi et al., 2004). Briefly, cortices were dissected in ice-cold Neurobasal medium (GIBCO) and incubated in 0.25% trypsin-EDTA (GIBCO) for 15 min in a 37°C water bath. The cells were then centrifuged and washed in Neurobasal medium containing 10% FBS, 0.25% L-Glutamine and 1% Penicillin-Streptomycin (all from GIBCO) and centrifuged again. The cells were resuspended in medium and gently mechanically triturated with a pipette, and allowed to stand for 15 min. The resultant supernatant was discarded, and the cells were resuspended in the abovementioned medium further supplemented with 2% B27 serum-free supplement (GIBCO). The cells were plated at 5×10^5 cells/dish in 35 mm dishes containing coverslips coated with poly-L-lysine (PLL), or at 1×10^5 cells/dish into PLL-coated or PA gel-coated confocal dishes. After 24 h, the medium was changed to Neurobasal + 2% B27 + 0.25% L-Glutamine + 1% Penicillin-Streptomycin. The medium was half-changed every 72 h.

METHOD DETAILS

Plasmid transfection

293T cells were seeded into 35 mm culture dishes at 1×10^6 cells per dish. The next day, the cells were transfected using the Lipofectamine 3000 kit (Invitrogen). 2.5 μg plasmid (replaced with water for the mock condition), 5 μl of P3000 and 5 μl of Lipofectamine 3000 were complexated according to the manufacturer's instructions, and added to the cells. 24 h later, the transfected cells were trypsinised and reseeded, partially into glass-bottomed confocal dishes (SPL Life Sciences) at 1/8 cell density, and partially back into the original dish. Live cells were photographed using a Nikon Eclipse TS100-F microscope 24 h later, and were then used for further experiments.

Preparation of PA hydrogels for neuron culture

Some confocal dishes were coated with a polyacrylamide (PA) hydrogel of a known stiffness much lower than that of glass using a previously-detailed protocol (Tse and Engler, 2010). Briefly, Confocal dishes were rinsed with 0.1 M NaOH, dried, incubated for 5 min with 3-aminopropyltriethoxysilane (Pierce Biotechnology), washed with distilled water, incubated with 0.5% glutaraldehyde for 30 min, and air-dried. A polyacrylamide gel solution was then added to the dishes such that the gel's final thickness would be 500 μm, and a coverslip was gently laid on it. The solution contained APS, TEMED, and acrylamide and bis-acrylamide (all from Pierce Biotechnology) at a ratio such that the polymerized gel would have a stiffness of 1 kPa (Tse and Engler, 2010). The gels were allowed to polymerize, the coverslips removed, and the dishes were thrice washed with PBS. The gels were then functionalized by adding a sulfo-SANPAH (Pierce Biotechnology) solution and exposing them to UV light of 320 or 365 nm to covalently link the gel to the sulfo-SANPAH. Next, the dishes were sterilized by UV light in a cell culture hood for 30 minutes, sealed, and stored at 4°C until required.

Viruses

We obtained high-titer viruses from commercial sources, and all viral aliquots were placed at −80°C prior to use. We used an rAAV-9 vector, with a human synapsin (hSyn) promoter, which enabled the viruses to preferentially transduct neurons, or a CaMKIIα promoter which preferentially transducted only excitatory neurons. The MscL-G22S sequence was fused with either the fluorescent reporter EYFP or the Ca^{2+} sensor protein GCaMP6S, and a polyA or 3x FLAG tag at the end of the sequence. In addition to the MscL-containing viruses, we also used vector controls. The viruses used in this study were rAAV/9-hSyn:EYFP-WPRE-pA, rAAV/9-hSyn:MscL-G22S-WPRE-EYFP-pA, rAAV/9-hSyn:MscL-G22S-GCaMP6S-WPRE-pA, rAAV/9-hSyn:GCaMP6S-WPRE-pA (all 4 purchased from BrainVTA (Wuhan) Co. Ltd.), pAOV/CaMKIIa-MscL-G22S-EYFP-3FLAG and pAOV/CaMKIIa-EYFP-3FLAG (both purchased from OBiO Technology, Shanghai).

Viral transduction

Primary neurons were transducted with at DIV 7 using viruses diluted 1/100 in PBS at RT. For every 5×10^5 primary neurons seeded, 10^9 genome copies (GC) of the CTRL virus and 10^{10} GC of the MscL-G22S virus were added directly into the cell medium. The plates were gently shaken and placed in the incubator. Cells were allowed to incubate for between 3-5 days while being monitored for fluorescence and cell condition, and then used in further experiments.

In vitro ultrasound stimulation system and protocol

The ultrasound stimulation system used in the present study was as illustrated in detail previously (Qiu et al., 2019). Briefly, it consisted of a commercial transducer (I7-0012-P-SU, Olympus), two function generators, and a power amplifier (Electronics and Innovation, A075) to produce 200 tone burst pulses at a center frequency of 500 kHz and a pulse repetition frequency (PRF) of 1 kHz with a duty cycle of 40%. The output intensity was limited to 0.05 - 0.5 MPa, with an interval of 10 s between pulses. The stimulation duration was 300 ms with 300 μs pulse width, except for primary neurons seeded on PA hydrogels, for which the pulse duration was 500 μs and the interval was 3 s. These parameters are similar to those that have been reported to effectively evoke behavior responses (Tufail et al., 2010).

Patch clamp

The resting membrane potentials of primary cortical neurons were recorded on DIV 14, 7 days after virus transduction. Borosilicate glass-made patch pipettes (Vitrex, Modulohm A/S, Herlev), were pulled with micropipette puller (P-97, Sutter Instrument Co.) to a resistance of 5–7MΩ after being filled with pipette solution. Current clamp was used for resting membrane potential in primary neurons. Once the membrane was broken, the value for resting membrane potential was noted. Digidata 1440B (Axon Instruments) and amplifier (Axopatch-700A, Axon Instruments) were applied for data recording with pClamp Version 9 software. The data were analyzed with Clampfit 10.0. Cells were bathed in a solution with 130 mM NaCl, 5 mM KCl, 1 mM $MgCl_2$, 2.5 mM $CaCl_2$, 10 mM glucose and 20 mM HEPES (pH 7.4). Pipettes were filled with a solution containing 138 mM KCl, 10 mM NaCl, 1 mM $MgCl_2$ and 10 mM HEPES with D-mannitol compensated for osm 290 (pH 7.2).

Calcium imaging

Cells were loaded with the fluorescent calcium indicator Fura-2 AM (F-1221, Invitrogen) according to the manufacturer's instructions, or primary neurons at DIV 10-12 expressing GCaMP6S, were used. For primary neurons seeded on PA hydrogels, the dye X-Rhodamine AM (X-14210, Invitrogen) at 4 μM was loaded into cells by incubating at 30 min at 37°C.A customized calcium imaging and ultrasound stimulation system was utilized. The system consisted of a modified upright epifluorescence microscope. The excitation light was generated by switchable LED light source (pE-340fura, CoolLED system), filtered by excitation filters and delivered to the sample for illuminating the calcium sensor. The fluorescence signals from the cells were collected by a water immersion objective (UMPlanFLN, Olympus), filtered by a filter wheel with green (525 nm) or red (633 nm) channels and captured by a sCMOS camera (ORCA- Flash4.0 LT Plus C114400-42U30, Hamamatsu). To minimize phototoxic effects, the LEDs were triggered at 1 Hz and synchronized with sCMOS time-lapse imaging. a triangle waveguide was attached to the ultrasound transducer and placed under the culture dish at a 45-degree angle to the horizontal axis. For Fura-2 imaging, dual excitation 340nm/380nm lights were inter-switched at 1 Hz, the calcium signaling were measured as the ratio of the signals at 340 nm and 380 nm. The other site of the waveguide was mounted with an acoustic absorber to minimize acoustic reverberation. During calcium imaging, the cells were placed in a buffer solution with 130 mM NaCl, 2 mM $MgCl_2$, 4.5 mM KCl, 10 mM Glucose, 20 mM HEPES, and 2 mM $CaCl_2$, pH 7.4.

RNA extraction and reverse-transcription

RNA was collected from cells using the GeneJET RNA Purification Kit (Thermo Scientific) according to the manufacturer's instructions, and RNA concentrations were measured using a NanoDrop One (Thermo Scientific). 1 μg RNA was reverse-transcribed using the iScript gDNA Clear cDNA Synthesis Kit (Bio-Rad), according to the manufacturer's instructions (including a gDNA digestion step), using a C1000 Touch thermal cycler (Bio-Rad).

Real-time qPCR

1 μL cDNA from plasmid-transfected 293T or virus-transducted primary neurons at DIV 12 was mixed with appropriate forward and reverse primers (final concentration 250 nM), 2X SYBR Green Premix *Ex* Taq (Takara) and H_2O to a final volume of 10 μl. PCR was performed using the CFX96 Touch Real-Time PCR Detection System (Bio-Rad). qPCR data were quantified using the CFX Maestro software (Bio-Rad). Results are expressed as a fold change compared to the appropriate control, mean ± SD of 3 independent experiments. Primer sequences were as follow:

Mouse β-actin: F - AGG GTG TGA TGG TGG GAA TG, R - TGG CGT GAG GGA GAG CAT AG, 402 bp; human β-actin: F - GTGGGGCGCCCCAGGCACCA, R - CTCCTTAATGTCACGCACGATTTC, 539 bp; MscL-G22S: F – GTCTCTTCACTGGTTGCCGA, R – TGCATCACAACAGCAGGGAT, 125 bp.

Immunocytochemical fluorescent staining

Primary neurons transducted with viruses were fixed at DIV 12 using 4% paraformaldehyde + PBS and permeabilized using 0.1% Triton X-100 + PBS. Cells were blocked using 5% normal goat serum in TBST and incubated overnight in primary antibodies diluted in 5% BSA + TBST. Secondary antibody incubation was performed the next day, diluted in 3% BSA in PBST for 1 h at room temperature. Cells were washed, coverslips dried, and mounted on glass slides using small drops of Prolong Glass Antifade Mountant with NucBlue (Life Technologies) and allowed to cure overnight at room temperature. All steps from the secondary antibody incubation onward were performed in the dark. Coverslip edges were then sealed using transparent nail enamel and imaged using a confocal laser scanning microscope (TCS SP8, Leica), at the University Research Facility in Life Sciences (ULS), The Hong Kong Polytechnic University.

MAP2 primary antibody (PA1-10005, Invitrogen) and goat anti-chicken IgY (H+L) Alexa Fluor 633 (A-21103, Invitrogen) were used at a dilution of 1:1000.

Stereotaxic injection

C57BL/6 mice were anesthetized with ketamine and xylazine (100 mg/kg and 10 mg/kg respectively) followed by shaving the skin above chosen cortical region (approximately corresponding to the right M1) or the dorsomedial striatum (DMS) area. Using the stereotaxic apparatus, a hole was drilled to allow injection. The coordinates used for cortical injection were AP 0.25 mm, ML-1.50 mm, DV 1.00 mm. The coordinates for DMS injection were AP 0.50 mm, ML −1.50 mm, DV −3.00 mm. Injection sites variously received 1 μl of rAAV/9-hSyn:MscL-G22S-EYFP-pA, rAAV/9-hSyn:EYFP-pA virus, pAOV/CaMKIIa-MscL-G22S-EYFP-3FLAG or pAOV/CaMKIIa-EYFP-3FLAG viral particles (2-3 × 10^{12} GC/ml) or saline (for sham experiments) at 0.1 μl/min, followed by a ten-minute pause. The pipette was then retracted slowly, including a five-minute pause at the halfway point. The puncture site was then disinfected and sutured, and the mice were returned to their housing areas.

EMG recording in anesthetized mice and data processing

Four weeks post-injection, 6 mice with CaMKII-promoted empty or MscL-G22S viruses in their right M1 regions each were anesthetized with 2% isoflurane and eye ointment applied to both eyes. Ultrasound gel was applied to the shaved head and a 500 kHz transducer was placed in contact with the gel. Two EMG electrodes were inserted approximately 3-5 mm apart into the tricep muscle of the left forelimb to record bioelectric potential difference across the muscle tissue. An EMG ground wire was attached to the tail of the animal. Isoflurane levels were reduced to 0.5% 5 min before starting EMG recording. Five rounds of ultrasound stimulation (500 kHz of 200 tone burst pulses, 300 ms stimulation duration, 400 μs pulse width. 1 kHz PRF, 40% duty cycle peak positive pressure 0.07 – 0.5 MPa) were performed on each subject. Each round consisted of 7 – 10 ultrasound stimuli delivered at an interval of 5 s. Each mouse was allowed 1 min rest between multiple rounds of stimulation. EMG signals were collected with a multi-channel signal acquisition system (Medus, Bio-Signal Technologies).

EMG data were analyzed using MATLAB (The MathWorks, Inc.). Raw EMG data were filtered using a 50 Hz notch and a 10 −150 Hz bandpass filter. A 200 ms window and the start of the recording was selected as a 'quiet period', and the data from the stimulation period were rectified about the mean of the filtered data. The data were smoothed using the upper root-mean-square envelope with a 200 ms sliding window. The mean of rectified data within the quiet period was treated as the signal baseline for the recording. 1.2 times the baseline was set as the threshold, and any signal rising above this level for minimum of 40 ms was considered a 'spike'. Within a post-stimulation window of 2.5 s following each ultrasound stimulus, if the first spike had a full-width-at-half-maximum, or a width above threshold for at least 100 ms, the spike was identified as a successful ultrasound-induced EMG event. The 'success rate' of each ultrasound stimulus was then calculated. Relative amplitude was calculated by the difference between the peak value of the identified EMG event and the signal baseline, divided by the same baseline ($\Delta A/A_{base}$). The response latency was measured as the time between delivery of ultrasound stimulus and the time-point at which the EMG signal rose above the threshold. Statistical significance of these data was determined using a two-tailed unpaired t test with Holm-Sidak correction. Standard error for the success rate was estimated by binomial proportion confidence interval using the normal approximation interval at the 95% confidence level.

Ultrasound stimulation in cortex and DMS

Five weeks post-injection, the mice were anesthetized by intraperitoneal injection of ketamine (100 mg/kg) and xylazine (10 mg/kg). Body weights were measured, the mice's heads were shaved, and ultrasound gel was applied there to promote acoustic coupling. The transducer was placed approximately above the M1 region (right forebrain) or above the DMS. Mice were stimulated with 0.3 MPa ultrasound (200 tone burst pulses with a center frequency of 500 kHz, PRF 1 kHz, 40% duty cycle, 300 ms stimulation duration, 400 μs pulse width) for 40 min with a 10 s stimulation interval. After stimulation, the mice were returned to their original cage.

Immunohistochemical fluorescent staining

90 min after ultrasound treatment, mice were perfused with PBS, followed by 4% paraformaldehyde (PFA) (cat. no. P1110, Solarbio) in PBS. Coronal sections were prepared from brain regions spanning +0.1 mm to −0.8 mm of Bregma in mouse brains for cortical sections and spanning +0.20 mm to 1.0 mm of Bregma for DMS sections. Individual sections were prepared spaced 40 μm apart. After dissection, brains were post-fixed overnight in 4% PFA. Starting from the injection plane, coronal brain slices at a thickness of 40 μm were collected. Slices were blocked using and incubated overnight in primary antibody solution diluted in 1% normal

goat serum + 5% BSA + PBS + 0.3% Triton. Slices were then washed with PBS, incubated with secondary antibodies diluted in PBS for 2 h at room temperature. Slices were then washed, coverslips dried, and mounted on glass slides using small drops of Prolong Diamond Antifade Mountant with DAPI. Primary antibody used was c-Fos (2250, Cell Signaling Technology, dilution 1:500). Secondary antibody used was goat anti-rabbit IgG (H+L), Alexa Fluor 555 (A-21428, Invitrogen, dilution1:1,000). Each sample was divided into 3 sets and 1 set was used to stain for c-Fos expression. Each set contained 6-7 brain slices. The number of cells showing c-Fos signals (red) and DAPI (blue) were counted using ImageJ, and the number of c-Fos$^+$ cells per 733 × 733 μm slice were calculated. The counting of c-Fos$^+$ cells was single-blinded, performed by an experimenter who did not know the groups beforehand. All brain slices were imaged using the confocal microscope (TCS SP8, Leica) in the ULS facilities in The Hong Kong Polytechnic University. These results were statistically analyzed using two-way ANOVA with post hoc Tukey test, and p values below 0.05 were considered significant.

Electrophysiology of acute brain slices

Mice expressing MscL-G22S or control virus in their cortices were deeply anesthetized and decapitated. Their brains were quickly removed and placed in ice-cold artificial CSF (ACSF) containing 125 mM NaCl, 2.5 mM KCl, 11 mM D-glucose, 26 m $NaHCO_3$, 1.25 mM NaH_2PO_4, 2 mM $CaCl_2$, and 2 mM $MgCl_2$. The solution was bubbled with 95% O_2/5% CO_2 to maintain a pH of ~7.4. Coronal slices (300 μm) containing cortex were cut on a microtome (Leica VT1200S) and were stored for 30–45 min at 37°C in oxygenated ACSF and then kept at RT. Individual slices were transferred to a recording chamber and fully submerged in continuously perfused (2–3 ml/min) oxygenated ACSF maintained at ~34°C. Only neurons indicating successful viral transduction by EYFP expression were recorded. The resting membrane potential recordings were performed following the detailed protocol used by Zhang et al. .

QUANTIFICATION AND STATISTICAL ANALYSIS

All statistical tests in this study were performed using GraphPad Prism 8 for Windows. Details of the statistical analyses performed for each figure are provided in the figure legends and in STAR Methods. A p value of < 0.05 or below was considered statistically significant for all experiments.